An adiabatic silica taper based on two sequential tapering routines

S. AL-ASKARI[a], B. A. HAMIDA[a], S. KHAN[a], M.YASIN[b], S. W. HARUN[c], Z. JUSOH[d]
[a]*Electrical and Computer Engineering Department - International Islamic University Malaysia, Jalan Gombak, 53100 Kuala Lumpur, Selangor, Malaysia*
[b]*Department of Physics, Faculty of Science and Technology, Airlangga University, Surabaya (60115) Indonesia*
[c]*Photonics Engineering Laboratory, Department of Electrical Engineering, University of Malaya 50603 Kuala Lumpur, Malaysia*
[d]*Faculty of Electrical Engineering, Universiti Teknologi Mara (Terengganu), 23000 Dungun, Terengganu, Malaysia*

Microfiber-based devices have a great potential in many applications due to their extraordinary optical and mechanical properties. An adiabatic silica-based taper is required for most of the applications and thus, adiabaticity criterion has to be estimated and satisfied to avoid high optical loss emerging when taper's profile is not controlled properly. This requires obtaining propagation constants via solving boundary condition problem at each position along the taper. Yet, this procedure involves intensive computational and time-consuming solving of complex Maxwell vector equations. This paper proposed an efficient method to model the taper profile, evaluate the adiabaticity and simulate it using Finite Element Analysis software. The model facilitates design phase and optimize fabrication process for any fiber-based device. A slow gradual radius reduction rates can guarantee adiabatic profiles with the expense of longer transition sections. In miniature devices, such as sensors and micro-resonators, transition regions are preferable to be as short as possible while the narrow waist is preferred to be long and uniform. To balance between short transition preference and low loss condition, we proposed a design based on two tapering sequential routines. The simulation results confirmed our design adiabaticity. From the optical spectrum of the fabricated taper, it is found that the loss is less than 1dBm and the spectrum is not distorted.

(Received September 22, 2016; accepted October 10, 2017)

Keywords: Microfiber, Tapered fiber, Taper, Adiabaticity, FEA, COMSOL

1. Introducion

Recently, optical fiber-based devices have been attracting greater research consideration due to their preferential advantages over their electrical counterparts, such like their low cost, compact size, low noise, high sensitivity, wide bandwidth and immunity to electromagnetic interference, particularly in harsh environmental conditions. Therefore, they have been developed and implemented in several applications including, and not limited to, force measurement, strain caused, displacement made, bending occurred, pressure variations, acceleration, rotation, vibration, electric fields, magnetic fields, acoustics, temperature and humidity. When the diameter of a single-mode fiber is minimized to a few micron or nano scales, this device is referred to Micro- or Nano-diameter optical Fibers (MNFs). Due to miniature diameter, the original core vanishes and the original cladding becomes the new core of the MNF [1]. The surrounding medium becomes the new cladding, where a considerable fraction of light in the form of evanescent field propagates. The micro- and nano-wires inherit several advantages from optical fibers, such as low cost, low noise and immunity to electromagnetic interference (EMI). In addition, the MNF size reduction offers couple of extraordinary optical properties and characteristics including, and not limited to; strong light confinement, low propagation loss, large evanescent field, low bend loss and nonlinearity [2]. All these exceptional advantages and unique properties of MNFs made them a potential platform for high-Q resonators and sensing applications [3-6].

MNFs can be fabricated from several materials. Silica glass is considered as the most commonly used material for fabricating an MNF due to its low cost and easiness of fabrication. However, a variety of materials are used and reported in the literatures, such as phosphate, tellurite, lead silicate, bismuthate, chalcogenide glasses and polymers. There are several approaches to fabricate a micro- or a nano-wire in the literatures and they can be classified into two categories; Bottom-Up and Top-Down techniques.

Optical fiber devices can be configured in several forms, such as: loops (MLRs) [7-9], knots (MKRs) [10], coils (MCRs) [11], Whispering Gallery Modes (WGMs) resonators [12], Mach–Zehnder interferometer [13], Fiber Bragg gratings (FBGs) [14] and microprobes [15]. COMSOL Multiphysics is utilized to evaluate the propagation constants as well as the effective indices of the fundamental mode propagating in different microfiber structures, such as; the optical coil resonator [16] and the optical loop resonator [8] for refractometric sensor applications. Ultra-high-Q micro-resonators based on

toroidal structure (micro-toroids) were also simulated to visualise the optical field intensity distribution [17].

The simplest structure is the straight MNF configuration where a single-mode fiber is tapered and this structure can be used as a sensor. In this case, the MNF is naturally connected to the pigtails. Another approach is to fabricate the MNF and then, to couple it evanescently to a taper. In both cases, low loss requirement is a must. Moldovean et al [18] obtained and illustrated propagation modes for different refractive indices of the core, core diameters, and wavelengths using a cross section model. On the other hand, The entire taper performance was studied based at different surrounding RI in [19] and different tapering ratios in [20].

In this paper, we proposed a new taper profile based on two tapering sequential routines. The proposed structure is then simulated using COMSOL Multiphysics to confirm our design adiabaticity. The taper has been also fabricated with the measured loss of less than 1dBm and the spectrum is not distorted. Next section will discuss the fundamentals of adiabaticity criteria. It is followed by taper model and taper design. The fifth section illustrates the simulation method followed in this study. Furthermore, the fabrication technique adopted is discussed in the sixth section. Finally, the results are presented and the work is concluded.

2. Adiabaticity criteria

The taper structure comprises of a narrow middle segment (taper waist) connected to the regular single-mode optical fiber (SMF) through conical sections (taper transitions), as shown in Fig. 1. Transition sections play an important role in transforming the fundamental core-cladding mode in the un-tapered SMF to the cladding-surrounding mode in the tapered waist. Higher order modes could survive, combine and interfere with the fundamental mode resulting in insertion loss. Coupling between two different modes can occur when both modes have same azimuthal polarization direction. In other words, the fundamental mode is therefore likely to couple to the LP_{02} mode if the radius reduction rate is fast.

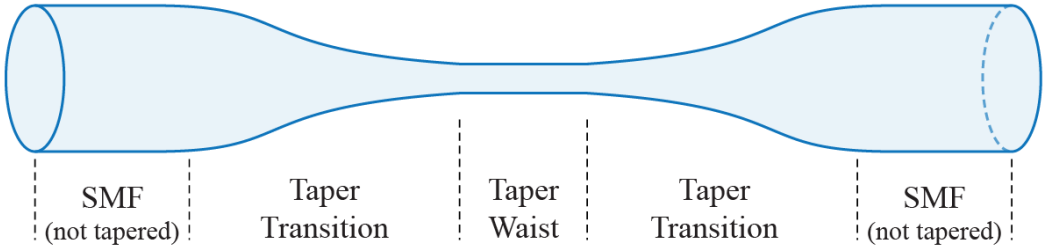

Fig. 1 Taper regions

The profile of transition sections has to be well optimized in order to reduce this interference, and consequently, to reduce the loss. This can be accomplished by reducing the taper diameter at slow gradual rates, which means longer transition sections. However, in miniature devices (such as in sensors and micro-resonators), transition regions are preferable to be as short as possible while the narrow waist is preferred to be long and uniform. To balance between short transition preference and low loss condition, transition has to be adiabatic at every point of it. Adiabaticity criterion was well studied and presented by Love et al. [21]. The length-scale condition;

$$z_t >> z_b \tag{1}$$

has to be satisfied everywhere along the taper in order to considered as an adiabatic taper. z_t is the local taper length-scale parameter and z_b is the polarization beat length, that is the coupling length between the fundamental mode and the second dominant local mode.

As illustrated in Fig. 2, z_t is the height of a cone whose circular base is the core cross section at z position, thus, we can write:

$$z_t = \frac{\rho}{\tan \Omega} \tag{2}$$

where ρ and Ω are the local core radius and the local taper angle at a position z. In practice, Ω is much less than 1, thus, tan (Ω) ≅ Ω. On the other hand, the coupling length between the two modes at z position is the polarization beat length between the fundamental mode and the second mode, and can be expressed as:

$$z_b = \frac{2\pi}{\beta_1 - \beta_2} = \frac{\lambda}{n_{eff1} - n_{eff2}} \tag{3}$$

where β_1 and β_2 are the propagation constants and n_{eff1} and n_{eff2} are the effective refractive indices of the fundamental and second mode, respectively. β_1 and β_2 can be evaluated at any each position by solving the Maxwell equations for a profile of a cylindrical fiber whose length is infinite, and its x-y dimensions match the taper cross-sectional geometry at position z, see the illustrated shaded orange cylinder in Fig. 2.

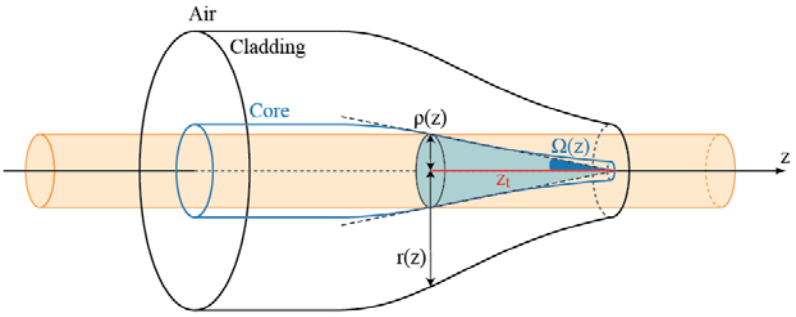

Fig. 2. An illustration of one side of the taper. The shaded orange cylinder is an infinite cylinder used to solve the electric field in order to find the propagation constants at position z

By applying (2) and (3) to the length-scale condition (1), we write:

$$\tan\Omega < \frac{\rho(\beta_1-\beta_2)}{2\pi} \tag{4}$$

$$\left|\frac{\delta\rho}{\delta z}\right| < \frac{\rho(\beta_1-\beta_2)}{2\pi} \tag{5}$$

where δρ/δz is the core radius reduction rate and its absolute value is equal to tan(Ω) at z position. To balance between radius reduction rate and taper length, equation (5) can be modified by replacing the core radius with the taper radius (r) and by introducing a factor f, such that, 0 < f < 1. The condition can be re-written as:

$$\frac{\delta r}{\delta z} < \frac{f\,r(\beta_1-\beta_2)}{2\pi} \tag{6}$$

In practice, tapers with negligibly low loss can be acquired with f = 0.5. However, the transition region length is about 2 times longer than that of optimal tapers obtained with f =1 [22].

2.1. Taper model

The model for the taper shape produced by thermal stretching is presented by Bricks and Li [23]. It is assumed that the taper is fabricated by heating and pulling its both ends apart equally, which means having a symmetric taper profile comprising of a waist and two identical transitions, as shown in Fig 1.

Inside the hot-zone, the fiber is a uniform cylinder of hot and softened glass whereas glass is cold and solidified outside the hot-zone. At any instant, the cylinder deforms to a longer and narrower cylinder with a length of L(t)+δx and a diameter of (rw+δrw), where δx >0 and δrw <0.

For a variable hot-zone length, the final waist radius for any x elongation can be expressed as:

$$r_w(x) = r_o\left[1+\frac{\alpha x}{L_o}\right]^{-1/2\alpha} \tag{7}$$

where r_o is the initial radius, L_o is the initial hot-zone length and α is the hot-zone variation parameter. We can also define the fiber radius at any position along the taper by relating the last equation to z instead of x:

$$r(z) = r_o\left[1+\frac{2\alpha z}{(1-\alpha)L_o}\right]^{-1/2\alpha} \tag{8}$$

This equation has been used in this study to estimate the taper profile before fabricating it. It is also used to model the taper using COMSOL Multiphysics. The problem is then solved using Boundary Mode Analysis, as discussed in the next section.

2.2. Taper design

The first step in taper design is to decide the final waist diameter and length based on the application. For instance, long waists are required for forming miniature structures. Generally, microfibers below 10 µm have large evanescent fields. However, very thin microfibers are extremely fragile. Thus, a final waist diameter of 6 µm is chosen in this work. α determines the rate by which hot-zone length changes. If α = +0.5 the taper transition has the shape of a reciprocal curve. If $\alpha \to 0$, transition region becomes exponential, as preferred [23].

Matlab is used to plot the equation (8) for α=0.2 and 0.5 as shown in Fig. 3. For α=0.2, an elongation of 5.9 cm is required to achieve the desired diameter and the waist length will be only 1.68 cm. In contrast, for α=0.5, an elongation of 19.5 cm is required and the waist length will be 10.25 cm. The first has a very short waist and the second is a very long taper and is hard to be handled. Thus, the two routines are better to be used sequentially.

Before the intersection point of the two graphs, the α=0.2 graph has a slow diameter reduction which is desirable for satisfying the adiabaticity criterion. Hence, it is suggested to start the tapering with α=0.2 routine until the intersection point, after which, tapering continues at α=0.5. The resulting taper, shown in Fig. 4, requires 6.2 cm elongation distance (1.75 cm of it at α=0.2) and it has 2.7 cm waist length. The straight segment between the two routines is because of the difference between the final hot-zone length of the first phase (which is 0.85 cm) and the initial hot-zone length of the second phase (which is 0.5 cm).

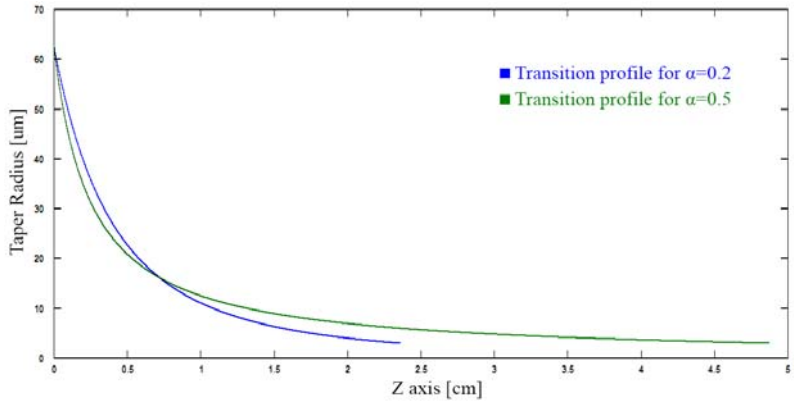

Fig. 3. The transition region profile of a taper whose waist diameter is 6 µm fabricated at different hot-zone variation parameters; α=0.2 (blue) and α=0.5 (green)

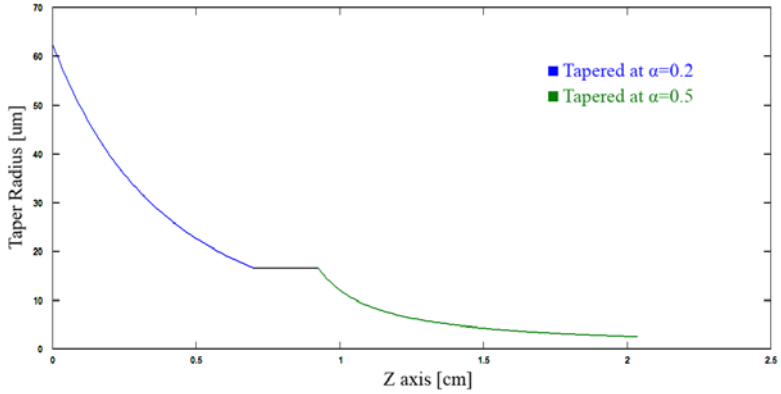

Fig. 4. The transition region profile of a taper whose waist diameter is 6 µm fabricated by sequential tapering routines; α=0.2 (blue) and α=0.5 (green)

The next step is to validate our design by simulating its cross section along the transition region to ensure its adiabaticity, as discussed in the following section.

2.3. Taper simulation

In the un-tapered fiber, the fundamental mode is confined in the core and the propagation constants will not change along the fiber. However, when entering the tapered region, the propagation constants for both fundamental mode and the second local mode will vary as the diameter of the cladding and the core vary. To find these constants, the boundary conditions can be solved using a 2D cross-section model of the core and the cladding in infinitely long cylindrical coordinates along the z axis of the taper. As the radius of the taper is extremely decreased, a third cylinder for air cladding is required. Eventually, the beat length zb can be found and compared to the local taper length-scale parameter zt to examine the taper adiabaticity.

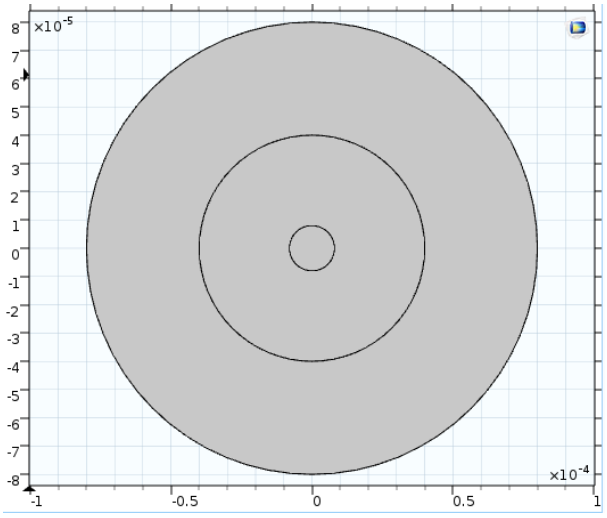

Fig. 5. A schematic diagram of the cross-sectional proposed model

The geometry of this model is pretty simple where three centralized circles are illustrated to define the three zones; core, cladding, and air. Fig. 5 shows a schematic diagram of the proposed model. The radii of both core and cladding are defined as functions of z based on equation (8) which gives the radius at any position z along the taper. The user can enter the desired elongation length in the parameter list and the final taper transition length zo will be calculated automatically based on the proper equations. A parametric sweep is applied on the parameter z over the range of 0 to zo. For each value of z, the geometry is modified accordingly and the model will represent the cross section of the taper at this position.

This model can also be used to find the propagation constants over a specific region of the taper transition zone by modifying Z and Zo values in the parameter list to the initial and final z values, respectively. For this physics interface, meshing plays an important role in solving the Mode Analysis where the maximum mesh element size has to be a fraction of the wavelength, at least one fifth the wavelength as COMSOL manual suggests.

2.4. Taper fabrication

The taper fabrication is an important process in any optical device development procedure. It has to be carried out systemically, thus, a high quality taper can be produced. A microfiber is considered as a high quality microfiber if it has the following properties: smooth surface, uniform waist diameter, large evanescent field, and low loss. The flame-brushing technique is one of the top-down heat stretching approaches, where the fiber is heated and stretched to minimize its diameter. It is initially demonstrated by [24] to fabricate optical directional couplers and it is then explored and used extensively in the field of microfiber applications. It is generally preferable due to its flexibility in producing desired taper profiles, i.e. its waist diameter, its waist length and its transition region length with accepted reproducibility and accuracy. Moreover, when a single-mode fiber (SMF) is tapered, the output microfiber becomes naturally connected to the regular SMF. This has a unique importance of offering an efficient light insertion and collecting with almost no loss.

Fig. 6 shows a picture of system diagram of tapering station, where an uncoated segment of fiber is placed horizontally between two fiber holders. One of these holders is movable on a linear stage and is controlled by a stepper motor. The uncoated segment of fibre is brushed by moving a flame back and forth along the segment. Thus, a burner is mounted on a sliding stage that is higher than that in the linear stage velocity in order to provide a uniform hot zone to the targeted region while it is being pulled. The sliding stage is controlled by another stepper motor and both motors are driven by a PIC microcontroller-based driving interface circuitry. The microcontroller is connected to a UART programmer linked to a personal computer. A mixture of oxygen and butane gases, and its pressure is controlled by valves, supplies the burner. During tapering process, transmission spectrum is monitored by injecting one end of the fiber by a wideband ASE (Amplified Spontaneous Emission) source and visualizing the output by connecting the other end of the fiber to an OSA (Optical Spectrum Analyser).

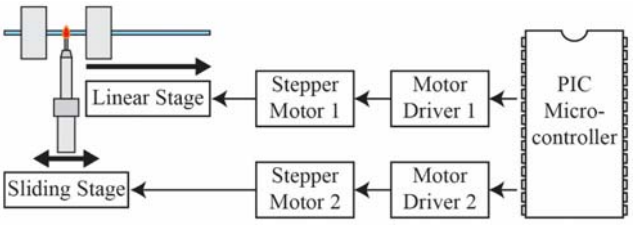

Fig. 6. System diagram of the motor control system

3. Results and discussion

When studying the adiabaticity along the taper, the effective mode indices or the propagation constants of the first two local modes have to be determined at each position. The mode analysis is set to search for modes around the refractive index of the core and the analysis frequency is set to c_const/wl, where c_const is the speed of light in vacuum and wl is 1.55 [μm]. Before tapering, the SMF is a straight step-index fiber where the fundamental mode is confined in the core and its neff is found equal to 1.4422. On the other hand, the second local mode is propagating along the core-cladding interface with an effective mode index of 1.438. The electric field distribution and its polarization direction for these modes are shown in Fig. 7.

The taper waist has a cladding radius of 3 [μm] acting as a new core. However, the radius of the original core is reduced in the model into 0.2 [μm] and is likely to be vanished in practice. To explore the impact of the original core in the microfiber simulation, we can simulate two cross sections of the waist with and without the core domain in the model. It is found that neff1 = 1.4322 and neff2 = 1.4137 in both cases. The electric field distribution is shown in Fig. 8. In Fig.8(a), the small circle in the centre of the MNF core illustrates the miniature original core. It is also interesting to notice the outer glow surrounding the MNF core and representing the evanescent field propagating in the air.

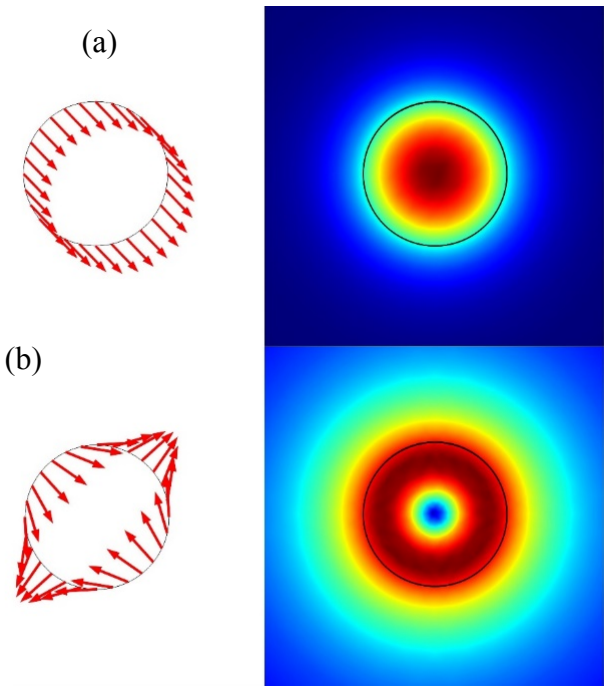

Fig. 7. The surface plot of the norm electric field of the SMF for: (a) n_{eff1} = 1.4422 and (b) n_{eff2} = 1.438

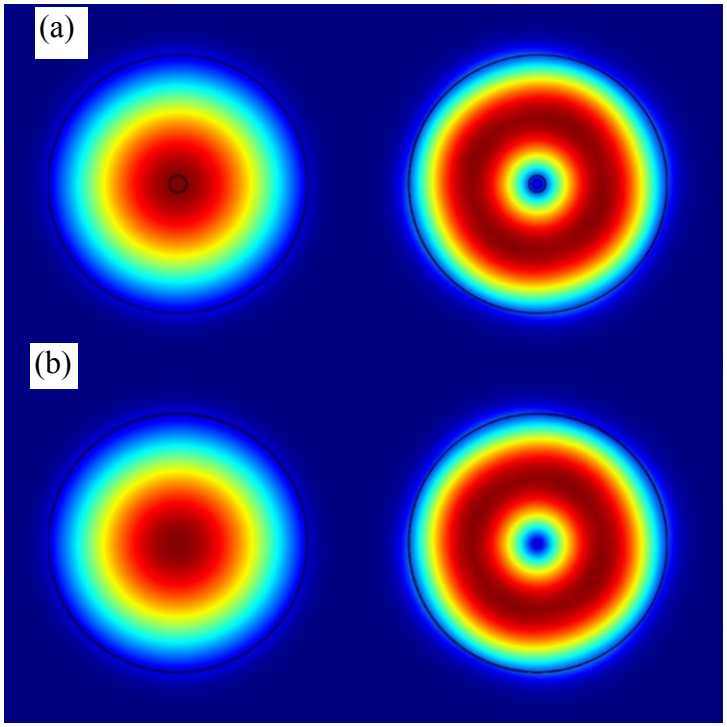

Fig. 8. The surface plot of the norm electric field of the taper waist for: n_{eff1} =1.4322 (left) and n_{eff2} = 1.4137 (right) with (a) and without (b) the core domain

The next study is to apply a parametric sweep of Z from 0 to 0.7 [cm] along the transition resulted from the first tapering routine. With a step of 100 [μm], the mode analysis of each cross section along the taper has been carried out. The output values of the effective refractive indices and the local core radius have been used to find the local taper length z_t and the beat length z_b. The adiabaticity condition can be examined through plotting and comparing z_t and z_b values along the first transition region, as shown in Fig. 9. There are distortions in both curves at 4.3 mm, which is most probably due to measurement errors.

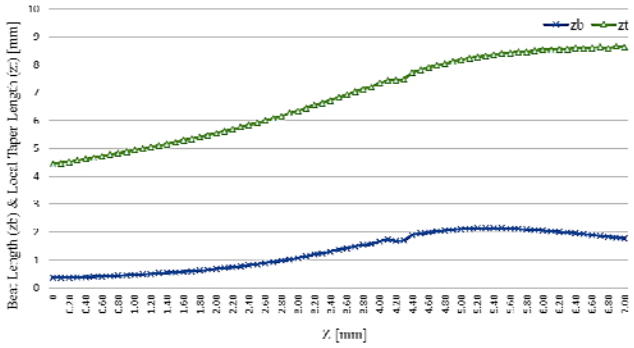

Fig. 9. The local taper length z_t and the beat length z_b along the first transition region

It is obvious that the taper is adiabatic for the first transition region since $z_t >> z_b$ condition is satisfied. By changing the hot-zone variation parameter α to 0.5 and applying another parameter sweep for Z (0 to 11.125 mm), the second transition region can be examined. Once again, z_t is larger than z_b along this region and the whole taper is confirmed to be adiabatic. The transmission optical spectra from a standard SMF (before tapering), adiabatic and non-adiabatic tapers are recorded and plotted in Fig. 10.

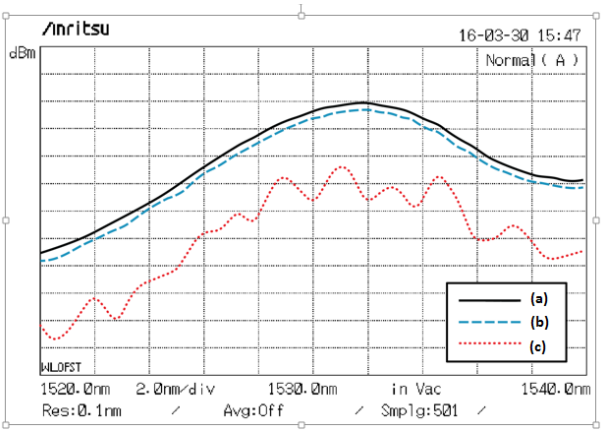

Fig. 10. Transmission spectrum of (a) SMF, (b) adiabatic taper, and (c) non-adiabatic taper

The SMF is tapered using the design parameters as previously described. As shown in the figure, the measured loss of the adiabatic taper is less than 1 dBm and the transmission spectrum is not distorted. However, the spectrum is distorted with a high loss (larger than 10 dB) for non-adiabatic taper. This taper is considered as a low quality taper, which promotes interference. In the non-adiabatic taper, some of the light beam leaks out into the cladding and thus the interferences between the core and cladding modes produces a comb filter as shown in Fig. 10. The microscopic images of the fabricated taper and the original SMF are shown in Fig. 11 (a) and (b), respectively.

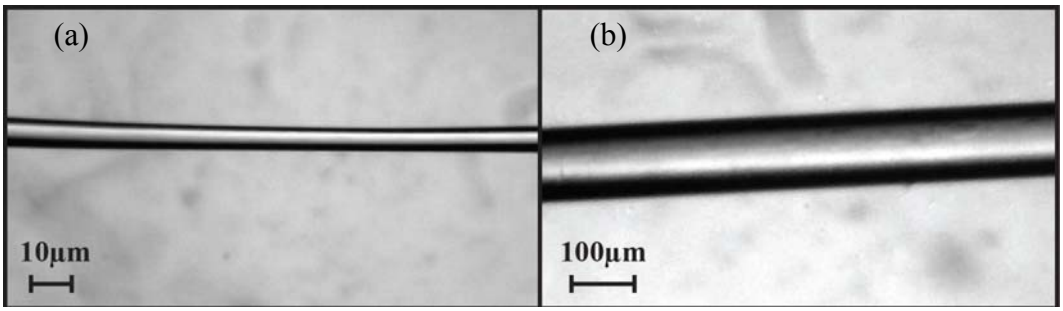

Fig. 11. Microscopic images of (a) Silica taper and (b) SMF

4. Conclusion

A low loss taper is an essential criterion in all-fiber micro devices applications where tapers are used for light coupling evanescently or for miniature structure construction. We proposed a method to model the taper and to simulate it to figure out its quality before fabrication. This method involved mode analysis of the cross section of the taper at all positions along the taper. Several plots were successfully produced to confirm taper's adiabaticity. The simulation results showed that the proposed taper design has a neglected loss. Our proposed design depended on two tapering sequential routines. These routines were applied practically and the output taper was adiabatic, as estimated.

Acknowledgement

This work is financially supported by Ministry of Higher Education (FRGS/1/2015/SG02/UITM/03/3) and PPP University of Malaya Grant Scheme (PG008-2016A).

References

[1] R. G. Hunsperger, Photonic devices and systems, New York: Marcel Dekker, 1994.
[2] G. Chen, M. Ding, Open Opt. J. **7**, 32 (2013).

[3] A. A. Jasim, M. Z. Muhammad, A. Z. Zulkifli, F. Ahmad, H. Ahmad, S. W. Harun, Optoelectron. Adv. Mat. **6**, 7 (2012).
[4] F. Wei, A. K. Mallik, D. Liu, Q. Wu, G. -D. Peng, G. Farrell, Y. Semenova, Scientific Reports **7**, 4725 (2017).
[5] J. Tian, S. Liu, W. Yu, P. Deng, Photonic Sensors **7**, 44 (2017).
[6] V. John, M. Z. Muhammad, N. Irawati, N. M. Ali, S. W. Harun, J. Optoelectron. Adv. M. **17**, 1656 (2015).
[7] M. Sumetsky, Y. Dulashko, J. M. Fini, A. Hale, Appl. Phys. Lett. **86**, 1 (2005).
[8] F. Xu, V. Pruneri, V. Finazzi, G. Brambilla, Opt. Express **16**, 1062 (2008).
[9] X. Guo, L. Tong, Opt. Express **16**, 14429 (2008).
[10] Y. Wang, H. Zhu, B. Li, Opt. Commun. **284**, 3276 (2011).
[11] Y. Hsieh, T. Peng, L. A. Wang, IEEE Photonics Technology Letters **24,** 569 (2012).
[12] G. C. Righini, Y. Dumeige, P. Féron, M. Ferrari, G. N. Conti, D. Ristic, S. Soria, Riv. del Nuovo Cim. **34,** 435 (2011).
[13] J. Wo, G. Wang, Y. Cui, Q. Sun, R. Liang, Opt. Lett. **37**, 67 (2012).
[14] W. Liang, Y. Huang, Y. Xu, R. K. Lee, A. Yariv, Appl. Phys. Lett. **86**, 1 (2005).
[15] Y. Tai, D. Chang, M. Pan, D. Huang, P. Wei, Sensors **16**(3), 303 (2016).
[16] C. Han, H. Ding, F. Lv, Sci. Rep. **4**, 7504 (2014).
[17] H. S. Choi, X. Zhang, A. M. Armani, Optics Letters **35**, 459 (2010).
[18] I. Moldovean, I. G. Tarnovan, Analysis Of Linearly Polarized Modes, COMSOL Conf. 2012 Bost., 2012.
[19] L. W. Li, X. H. Sun, Investigation on the tapered fiber evanescent-field sensor based on the comsol software, in 2012 Symposium on Photonics and Optoelectronics, SOPO 2012, 2012.
[20] S. Al-Askari, B. A. Hamida, S. Khan, S. W. Harun, ARPN Journal of Engineering and Applied Sciences **11**, 449 (2016).
[21] J. D. Love, W. M. Henry, W. J. Stewart, R. J. Black, S. Lacroix, F. Gonthier, Tapered single-mode fibres and devices. Part 1: Adiabaticity criteria, October, 1991.
[22] S. W. Harun, K. S. Lim, C. K. Tio, K. Dimyati, H. Ahmad, Optik **124**, 538 (2013).
[23] T. A. Birks, Y. W. Li, J. Light. Technol. **10**, 432 (1992).
[24] F. Bilodeau, K. O. Hill, S. Faucher, D. C. Johnson, J. Light. Technol. **6**, 1476 (1988).

*Corresponding author: swharunt@um.edu.my